Development 137, 4177-4189 (2010) doi:10.1242/dev.048827

Pak1 control of E-cadherin endocytosis regulates salivary gland lumen size and shape

Carolyn Pirraglia*, Jenna Walters and Monn Monn Myat†

SUMMARY

Generating and maintaining proper lumen size and shape in tubular organs is essential for organ function. Here, we demonstrate a novel role for p21-activated kinase 1 (Pak1) in defining the size and shape of the *Drosophila* embryonic salivary gland lumen by regulating the size and elongation of the apical domain of individual cells. Pak1 mediates these effects by decreasing and increasing E-cadherin levels at the adherens junctions and basolateral membrane, respectively, through Rab5- and Dynamin-dependent endocytosis. We also demonstrate that Cdc42 and Merlin act together with Pak1 to control lumen size. A role for Pak1 in E-cadherin endocytosis is supported by our studies of constitutively active Pak1, which induces the formation of multiple intercellular lumens in the salivary gland in a manner dependent on Rab5, Dynamin and Merlin. These studies demonstrate a novel and crucial role for Pak1 and E-cadherin endocytosis in determining lumen size and shape, and also identify a mechanism for multiple lumen formation, a poorly understood process that occurs in normal embryonic development and pathological conditions.

KEYWORDS: Cadherin, Endocytosis, Pak, Rab5, Salivary gland, Lumen and tube morphogenesis, Cdc42, Merlin, *Drosophila*

INTRODUCTION

Tubular networks provide structure and function for many essential organs, such as the vasculature, gut, lung and kidney. Tube formation occurs through a complex series of events including cell shape changes, cell migration and changes in cell adhesion (Lubarsky and Krasnow, 2003; Martin-Belmonte and Mostov, 2008). Central to the morphogenesis of tubular organs is the formation of a lumen of the correct size and shape that mediates the delivery of gases and nutrients or the removal of waste. Failure to achieve and/or maintain correct lumen size and shape can lead to pathological conditions such as polycystic kidney disease and stenoses. Lumens can form by a number of mechanisms, such as through folding, as occurs in the mammalian and avian neural tube, or de novo through apoptosis and autophagy, as occurs in the mammary and submandibular glands (Colas and Schoenwolf, 2001; Debnath and Brugge, 2005; Mailleux et al., 2008; Melnick and Jaskoll, 2000). Lumens can also form de novo by the formation and coalescence of intracellular vesicles, as occurs in zebrafish vasculature and cultured endothelial cells (Kamei et al., 2006; Koh et al., 2008). Alternatively, lumens can form extracellularly between adjacent endothelial cells, as was recently demonstrated in the mouse aorta (Strilic et al., 2009).

Recent in vitro studies of lumen formation using cultured cells grown as cysts in three-dimensional matrices revealed an essential role for the Rho family GTPase Cdc42 in de novo lumen formation. In MDCK cysts, reduction of Cdc42 activity delayed single lumen formation and led to formation of cysts with multiple small lumens (Martin-Belmonte et al., 2007). Knockdown of Cdc42 in Caco-2 cells led to cysts with two or more lumens due to a defect in the orientation of the mitotic spindle (Jaffe et al., 2008). Although these studies provided mechanistic insight into Cdc42-dependent lumen formation in vitro, it is not known whether the same mechanism holds true for lumen formation in vivo in a developing tubular organ.

Pak proteins are a family of serine-threonine kinases known to bind and be activated by the Rho family GTPases Cdc42 and Rac to regulate a number of diverse biological processes, including cell migration and cytoskeletal rearrangements (Arias-Romero and Chernoff, 2008; Bokoch, 2003). Although much is known about the structure, biochemistry and cell biology of mammalian Paks, less is known about their biological role in vivo. Studies of cultured mammalian cells showed that Paks are required for lamellipodium extension and for disruption of E-cadherin-based cell-cell junctions (Kiosses et al., 1999; Lozano et al., 2008; Royal et al., 2000; Zegers et al., 2003). Mutations in zebrafish Pak2a cause loss of vascular integrity characterized by abnormally formed blood vessels (Buchner et al., 2007; Liu et al., 2007). In cysts formed from cultured endothelial cells, Pak proteins act downstream of Cdc42 to regulate de novo lumen formation (Koh et al., 2008; Koh et al., 2009). Thus, these studies suggest a crucial role for Pak kinases in tube and lumen morphogenesis; however, the mechanism by which Paks act is not known.

The *Drosophila* embryonic salivary gland is a genetically tractable model system for investigating tube and lumen morphogenesis. It consists of a pair of elongated epithelial tubes that are required for secretion during the larval stage. Each gland comprises a single layer of epithelial cells surrounding a central lumen. The gland lumen is formed during the process of invagination when primordial cells invaginate from the ventral surface of the embryo (Myat, 2005). Once internalized, gland cells undergo a phase of robust apical membrane growth that is regulated by the transcription factors Hairy, Huckebein (Hkb) and Ribbon, the apical membrane protein Crumbs, and a microtubule motor encoded by the *klarsicht* gene (Kerman et al., 2008; Myat and Andrew, 2002). As internalized gland cells begin to migrate

Department of Cell and Developmental Biology, Weill Medical College of Cornell University, 1300 York Avenue, New York, NY 10065, USA.

*BCMB Program of Weill Graduate School of Medical Sciences at Cornell University, New York, NY 10065, USA
†Author for correspondence (mmm2005@med.cornell.edu)

Accepted 7 October 2010

posteriorly, the expanded apical membrane is re-absorbed and the apical domain of each cell becomes elongated with its longest axis along the proximal-distal (Pr-Di) axis of the gland through an unidentified mechanism (Myat and Andrew, 2002).

A role for the *Drosophila* Pak4 homolog Mbt in the regulation of E-cadherin (Shotgun – FlyBase)-based adherens junctions and a role for *Drosophila* Pak1 (Pak – FlyBase) in apicobasal polarity and F-actin assembly have been demonstrated (Menzel et al., 2008; Menzel et al., 2007). Here, we demonstrate a novel role for *Drosophila* Pak1 in the control of salivary gland lumen size and shape through Merlin and Rab5- and Dynamin (Shibire – FlyBase)-mediated E-cadherin endocytosis.

MATERIALS AND METHODS

Drosophila strains and genetics

Fly lines used were: UAS-*Cdc42*^{L89}, *Pak3*^{LA00012}, *rab5*^{EY1069}, UAS-*Rab5*^{S43N}-YFP, UAS-*Rab5*^{Q88L}-YFP, UAS-*Rab4*^{S22N}-YFP, UAS-*Rab7*^{T22N}-YFP, UAS-*Rab11*^{S25N}-YFP, UAS-*shi*^{K44A}, UAS-*Rab4*^{WT}-YFP, UAS-*Rac1*^{N17}, *Df(3R)Win11*, *shg*^{2} (Bloomington Stock Center); UAS-*Rab5*^{WT}-GFP, UAS-*Rab7*^{WT}-GFP, UAS-*Rab11*^{WT}-GFP, UAS-*LAMP1*-GFP (C. Samakovlis, Stockholm University, Stockholm, Sweden); UAS-*E-cadherin*-GFP (H. Oda, Osaka University, Osaka, Japan); UAS-*p35* (H. Stellar, The Rockefeller University, New York, NY, USA); *fkh*-GAL4^{II}, *fkh*-GAL4^{III} (D. Andrew, Johns Hopkins University, School of Medicine, Baltimore, MD, USA); *Pak1*^{14}, *Pak1*^{4}, *Pak1*^{16}, *Pak1*^{6}, UAS-*Pak1*^{myr}, UAS-*Pak1*^{WT} *Pak1*^{6} (N. Harden, Simon Fraser University, Burnaby, B.C. Canada); UAS-*Mer*^{WT}-myc, UAS-*Mer*^{BBA}-myc (R. Fehon, The University of Chicago, Chicago, IL, USA). Canton-S flies were used as wild-type controls. The UAS-Gal4 system (Brand and Perrimon, 1993) was used with *fkh*-GAL4 to drive salivary gland-specific expression. Homozygous mutant embryos were distinguished by the absence of β-galactosidase staining, which detects the expression of *lacZ* from the *Ubx-lacZ* insert on the balancer chromosome.

Antibody staining of embryos

Embryo fixation and staining were performed as described previously (Pirraglia et al., 2006). Primary antibodies used were: anti-Phalloidin (AF488; Invitrogen; 1:200), rabbit anti-Avalanche (Syntaxin 7 – FlyBase; obtained from H. Kramer, UT Southwestern Medical Center, Dallas, TX, USA; 1:1000), chicken anti-Avalanche (obtained from D. Bilder, UC Berkeley, Berkeley, CA, USA; 1:500), mouse anti-β-galactosidase (Promega; 1:10,000 for whole-mount, 1:500 for immunofluorescence), rabbit anti-Bazooka (obtained from J. Zallen, Sloan Kettering Institute, New York, NY, USA; 1:1000), rat anti-CrebA (generated in the Myat Lab, New York, NY, USA; 1:10,000 for whole-mount, 1:5000 for immunofluorescence) (Andrew et al., 1997), rabbit anti-Croquemort (obtained from N. Franc, The Scripps Research Institute, La Jolla, CA, USA; 1:500), mouse anti-Crumbs [Developmental Studies Hybridoma Bank (DSHB); 1:100 for whole-mount, 1:10 for immunofluorescence], rat anti-E-cadherin (DSHB; 1:20), mouse anti-Discs large (DSHB; 1:500), rabbit anti-Engrailed (obtained from P. O'Farrell, UC San Francisco, San Francisco, CA, USA; 1:1000), rabbit anti-Fork head (obtained from M. Stern and S. Beckendorf, UC Berkeley, Berkeley, CA, USA; 1:1000), mouse anti-GFP (Roche Diagnostics; 1:500), mouse anti-Myc (Invitrogen; 1:500), mouse anti-Neurotactin (DSHB; 1:10), rabbit anti-Pak (obtained from N. Harden, Simon Fraser University, Burnaby, B.C. Canada; 1:2000), rat anti-PH4αSG1 (obtained from D. Andrew, Johns Hopkins University, School of Medicine, Baltimore, MD, USA; 1:5000), rabbit anti-Pio (obtained from M. Affolter, University of Basel, Basel, Switzerland; 1:200) and rabbit anti-aPKC (Santa Cruz Biotechnology; 1:500). The appropriate biotinylated- (Jackson Immunoresearch Laboratories), AlexaFluor (AF) 488-, AF546-, AF647- or Rhodamine- (Molecular Probes) conjugated secondary antibodies were used at a concentration of 1:500. 3,3′-Diaminobenzidine-stained embryos were mounted in methyl salicylate (Sigma) and visualized on a Zeiss Axioplan 2 microscope with Axiovision Rel 4.3 software (Carl Zeiss). Fluorescent embryos were mounted in Aqua polymount (Polysciences) and 1 μm sections were acquired on a Zeiss Axioplan microscope (Carl Zeiss) equipped with LSM 510 for laser scanning confocal microscopy at the Rockefeller University Bio-imaging Resources Center (New York, NY, USA).

Analysis of recombinant lines

Recombinant lines carrying different UAS-transgene insertions were confirmed by PCR analysis as described previously (Pirraglia et al., 2006).

Transmission electron microscopy of embryos

Embryos were processed for transmission electron microscopy (TEM) as described previously (Myat and Andrew, 2002). Thin serial sections were generated and analyzed on a Joel 100CX-11 Transmission Electron Microscope at the Weill Cornell University Microscopy Core Facility (New York, NY, USA). At least three embryos were analyzed for each genotype.

Morphometric analyses

The apical domain area of individual gland cells was measured by tracing E-cadherin (E-cad) immunofluorescent staining at the level of the adherens junctions (AJs) using LSM 510 Image Browser software (Carl Zeiss). The elongation ratio was determined by calculating the ratio of apical domain length oriented along the Pr-Di axis to the apical domain length along the dorsal-ventral (D-V) axis using LSM 510 software. The basolateral perimeter and domain areas of individual gland cells were measured by tracing F-actin staining of laterally viewed stage 13 embryos using LSM 510 software. Lumen length was determined by tracing E-cad-labeled lumens, and lumen width was determined by measuring lumen diameter of the proximal, medial and distal regions of the gland with LSM 510 software. At least five embryos were analyzed for each genotype and a maximum of three cells were measured per gland. Statistical analysis was performed using Microsoft Excel.

Fluorescence intensity analyses

Total fluorescence intensity of E-cad was quantified in embryos double-stained for E-cad and Crb or triple-stained for E-cad, aPKC and Nrt. Total fluorescence intensity of E-cad per apical domain was measured using NIH Image J software (http://rsb.info.nih.gov/ij/) and normalized against the total fluorescence intensity of Crb or aPKC. Total fluorescence intensity of E-cad per basolateral membrane was normalized against the total fluorescence intensity of Nrt. At least five embryos were analyzed for each specified genotype and a maximum of three cells were measured per gland. Statistical analysis was performed using Microsoft Excel.

RESULTS

To understand Pak1 function in salivary gland development, we analyzed an allelic series of *Pak1* zygotic loss-of-function mutations. The *Pak1*^{14} allele contains a premature stop codon within the Cdc42/Rac interactive binding (CRIB) domain and is considered to be a null allele; the *Pak1*^{6} allele contains a premature stop codon within the CRIB domain; the *Pak1*^{16} allele contains a premature stop codon between the CRIB domain and the kinase domain; and the *Pak1*^{4} allele contains a missense mutation in the PxxP domain, a proline-rich domain known to bind Nck (Dock – FlyBase) (Hing et al., 1999). In embryos homozygous for *Pak1*^{14}, gland lumens were expanded and irregular in shape, in contrast to lumens of heterozygous siblings (Fig. 1A-D). Consistent with their molecular lesions, gland lumen defects in *Pak1*^{16} homozygotes were milder compared with *Pak1*^{14} homozygotes but more severe compared with *Pak1*^{4} homozygotes (data not shown). We also observed mis-shapen lumens in glands of *Pak1*^{14}*Pak1*^{16}, *Pak1*^{14}*Pak1*^{4} and *Pak1*^{14}*Pak1*^{6} trans-heterozygous embryos; embryos trans-heterozygous for *Pak1*^{14} and *Df(3R)Win11*, a deficiency that completely removes the *Pak1* gene; and embryos mutant for another *Drosophila* Pak protein, Pak3 (see Fig. S1 in the supplementary material).

In addition to defects in gland lumen size, we observed defects in tracheal development, a network of interconnected epithelial tubes that, like the salivary gland, forms by invagination and

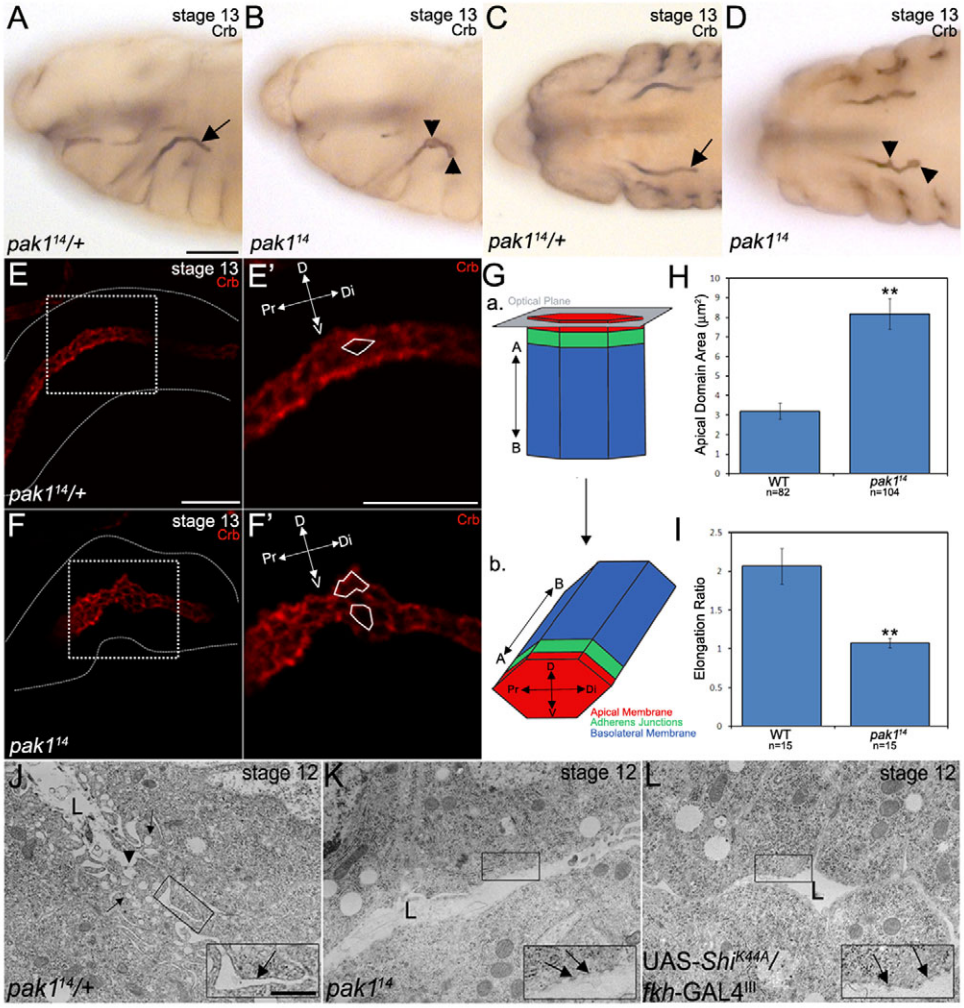

Fig. 1. Pak1 is required for correct lumen shape and size during salivary gland migration in *Drosophila*. (**A-F′**) Embryos were stained for Crb to label the apical membrane. In *Pak1*^{14} heterozygous embryos (A,C), glands migrate posteriorly to form elongated tubes (arrows), whereas in homozygous embryos (B,D), the gland lumen is irregular in shape and expanded (arrowheads). In *Pak1*^{14} heterozygous embryos (E,E′), Crb outlines the gland lumen and the apical domains of individual cells (solid white outline) which are smaller and more elongated in the Pr-Di axis, compared with homozygous siblings (F,F′; solid white outline). Dotted white lines in E and F outline the gland. E′ and F′ are magnified views of the dotted boxed regions in E and F, respectively. (**G**) Diagram of a lateral (a) and apical (b) view of a gland cell showing the apical (red) and basolateral (blue) membranes, adherens junctions (green) and the plane in which optical sections were acquired (gray) to measure the apical domain area and elongation ratio of individual cells. (**H**,**I**) Measurements of apical domain area (H) and elongation ratio (I) in wild-type and *Pak1*^{14} salivary gland cells. *n* represents the total number of cells scored per genotype, with a maximum of three cells measured per gland. Data are mean ± s.d. $^{**}P<0.005$. (**J-L**) In *Pak1*^{14} heterozygous glands (J), the apical membrane facing the lumen consists of numerous membrane extensions containing vesicular structures (small arrows), some of which are in contact with the lumenal space (arrowhead). In *Pak1*^{14} mutant glands (K), and glands expressing *shi*^{K44A} (L), the apical surface is devoid of membrane extensions and lacks vesicular structures, and instead is studded with electron-dense patches (arrows within insets in K and L) compared with wild type (arrow within inset in J), which has none. A, apical; B, basal; D, dorsal; Di, distal; L, lumen; Pr, proximal; V, ventral. Scale bars: 20 μm in A; 10 μm in E and E′; 1 μm in J.

migration. The lumens of *Pak1*^{14} mutant dorsal trunk and visceral branches were stalled and not extended like those of heterozygous siblings, suggesting a defect in tracheal migration and/or lumen extension; however, tracheal lumens were not expanded as in the salivary gland (see Fig. S2 in the supplementary material).

To understand how gland lumen size changes over the course of gland development, we measured lumen length and width in glands of wild-type embryos between stage 11 (after invagination is complete) to stage 13 (when glands have turned posteriorly). Lumen length more than tripled during this timecourse, whereas changes in lumen width varied; lumen width in the proximal region of the gland decreased the most over time, whereas no changes in lumen width were observed in the medial and distal portions of the gland (see Fig. S3B,C in the supplementary material).

During early development of wild-type glands, apical membrane growth accompanied elongation of the apical domain of individual gland cells with their longest axis being the Pr-Di axis (Myat and Andrew, 2002). To assess how changes in the apical domain contribute to the overall shape and size of the gland lumen, we measured changes in apical domain area and elongation. During invagination in early stage 11, gland cells had large apical domains; however, during gland turning (between

stages 12 and 13), cells progressively reduced their apical domain size (see Fig. S3D in the supplementary material). We also observed changes in apical domain shape during gland turning. In early stage 11 gland cells, the apical domain was isotropic, whereas during gland turning, the apical domain became anisotropic and was three times as long in the Pr-Di direction as in the D-V axis (see Fig. S3E in the supplementary material). After turning was complete, the apical domains became less anisotropic and were twice as long in the Pr-Di direction as in the D-V direction (see Fig. S3E in the supplementary material).

Loss of Pak1 function resulted in changes in gland lumen size. The gland lumen was wider in the medial and distal regions of *Pak1*^{14} mutant embryos compared with wild-type glands although lumen length was unchanged (see Fig. S4E,F in the supplementary material). Expanded gland lumens of *Pak1*^{14} mutant embryos did not arise from abnormal cell proliferation as determined by cell counting and staining for phosphorylated histone 1B (data not shown). Instead, increased gland lumen width was accompanied by a two- to three-fold increase in the apical domain area of individual gland cells with a concomitant failure to elongate their apical domains in the Pr-Di axis (Fig. 1E-H). Although apical domain size and elongation were dramatically altered in *Pak1*^{14} mutant gland cells, the perimeter of the basolateral membrane and the area of the basolateral domain were not affected (see Fig. S3F in the supplementary material).

To determine whether loss of Pak1 affected apical membrane topography, we performed transmission electron microscopy (TEM) of *Pak1*^{14} homozygous embryos. In the glands of *Pak1*^{14} heterozygous embryos that have completed invagination, highly irregular membrane extensions protruded into the lumen and contained vesicular structures, some of which were in contact with the lumenal space (Fig. 1J). By contrast, in the glands of *Pak1*^{14} homozygous embryos, the apical surface was devoid of membrane extensions and vesicular structures, and instead was characterized by electron-dense patches that resembled Dynamin-positive flat-coated surfaces at the plasma membrane of cultured mammalian cells (Fig. 1K) (Damke et al., 1994). Thus, in *Pak1* mutant gland cells, not only were the apical domains expanded and failed to elongate, but the topography of the apical surface membrane was also dramatically altered.

Pak1 functions in salivary gland cells to control E-cadherin localization

To determine whether remodeling of E-cadherin (E-cad)-based adherens junctions (AJs) plays a role in reorganization of the apical domain, we analyzed E-cad localization in wild-type and *Pak1*^{14} mutant gland cells. In contrast to wild-type gland cells where E-cad localized to the AJs and to the basolateral membrane (Fig. 2A), in *Pak1*^{14} mutant glands (Fig. 2B), E-cad localization at the basolateral membrane was lost, although it was still present at the AJs. Measurement of fluorescence intensity demonstrated that *Pak1*^{14} mutant gland cells contained more E-cad at the AJs and less at the basolateral membrane compared with heterozygous siblings (Fig. 2C,D); however, Crb levels were similar in *Pak1*^{14} homozygous and heterozygous embryos (data not shown), indicating that Pak1 specifically regulates E-cad at the AJs. The increased expression of E-cad in the AJs in *Pak1*^{14} mutant gland cells suggested that increased E-cad localization at the AJs might be responsible for the observed defects in apical domain size and elongation. Thus, we analyzed embryos homozygous for a zygotic hypomorph allele of *shotgun*, the gene which encodes E-cad, *shg*^{2}. In *shg*^{2} homozygous embryos, gland lumens were mis-shapen and expanded (data not shown); however, apical domain size was only slightly more expanded than that of wild-type cells and not expanded to the same extent as *Pak1*^{14} mutant cells (Fig. 2E). Moreover, E-cad was not localized at the basolateral membrane in *shg*^{2} mutant gland cells (data not shown) and apical domains were not elongated in the Pr-Di axis (Fig. 2F). In embryos trans-heterozygous for *Pak1*^{14} and *shg*^{2}, E-cad localized to the AJs and apical domain size was comparable with that of wild-type gland cells; however, E-cad was not found at the basolateral membrane and apical domains failed to elongate (Fig. 2E,F; data not shown). To test whether expansion of the apical domain in *Pak1*^{14} mutant gland cells was dependent on having normal levels of *shg*, we analyzed *Pak1*^{14} mutant glands that were also heterozygous for *shg*^{2} (*Pak1*$^{-/-}$;*shg*$^{+/-}$). The apical domain area of *Pak1*$^{-/-}$;*shg*$^{+/-}$ mutant gland cells was significantly reduced compared with *Pak1*^{14} homozygous mutants; however, the apical domains of *Pak1*$^{-/-}$;*shg*$^{+/-}$ gland cells were not elongated (Fig. 2E,F). From these data, we conclude that Pak1 limits the pool of E-cad at the AJs in order to restrict apical domain size, and promotes E-cad at the basolateral membrane, which correlates with elongation of the apical domain along the Pr-Di axis. These Pak1-mediated events are necessary for establishing the correct lumen size and shape in the salivary gland.

Endogenous Pak1 was expressed ubiquitously in the embryo and in gland cells, and was strongly expressed in the apical membrane and in sub-apical vesicles where it colocalized with the early endosome marker protein Avalanche (Aval; see Fig. S5 in the supplementary material). To demonstrate that Pak1 functions cell-autonomously in gland cells to regulate E-cad localization, we expressed wild-type Pak1 (*Pak1*^{WT}) specifically in the glands of *Pak1*^{14}*Pak1*^{6} trans-heterozygous (*Pak1*$^{14+/-}$*Pak1*$^{6+/-}$) embryos. In *Pak1*$^{14+/-}$*Pak1*$^{6+/-}$ embryos, apical domain size was expanded and apical domains failed to elongate, as was observed also in *Pak1*^{14} homozygous embryos (see Fig. S3G,H in the supplementary material). We observed a significant rescue of apical domain size and elongation, and basolateral localization of E-cad in *Pak1*$^{14+/-}$*Pak1*$^{6+/-}$ mutant glands expressing *Pak1*^{WT} compared with *Pak1*$^{14+/-}$*Pak1*$^{6+/-}$ mutant glands (see Fig. S3G,H in the supplementary material; data not shown). Thus, Pak1 is required in gland cells for generating proper lumen size and shape through differential localization of E-cad.

Cdc42 controls salivary gland lumen size

Since Pak proteins are activated by both Cdc42 and Rac small GTPases, we tested whether Cdc42 and/or Rac were required for correct gland lumen size and shape. We inhibited Cdc42 and Rac1 function specifically in the gland by expressing either dominant-negative Cdc42 (*Cdc42*^{DN}) or Rac1 (*Rac1*^{DN}) with the *fork head* (*fkh*)-GAL4 driver. *Cdc42*^{DN} expression led to expanded gland lumen width in the medial and distal regions similar to that observed as a result of loss of *Pak1* function, whereas *Rac1*^{DN} expression had no effect (see Fig. S4B,D,E in the supplementary material). *Cdc42*^{DN} expression had no effect on lumen length, as with loss of *Pak1* function; however, *Rac1*^{DN} expression led to formation of a shorter lumen that is likely to be a result of the role of Rac1 in gland migration that we reported previously (see Fig. S4F in the supplementary material) (Pirraglia et al., 2006). E-cad failed to localize to the basolateral membrane of gland cells expressing *Cdc42*^{DN}, as observed also in *Pak1*^{14} mutant gland cells (see Fig. S4B in the supplementary material). By contrast, E-cad localized prominently to the basolateral membrane of gland cells

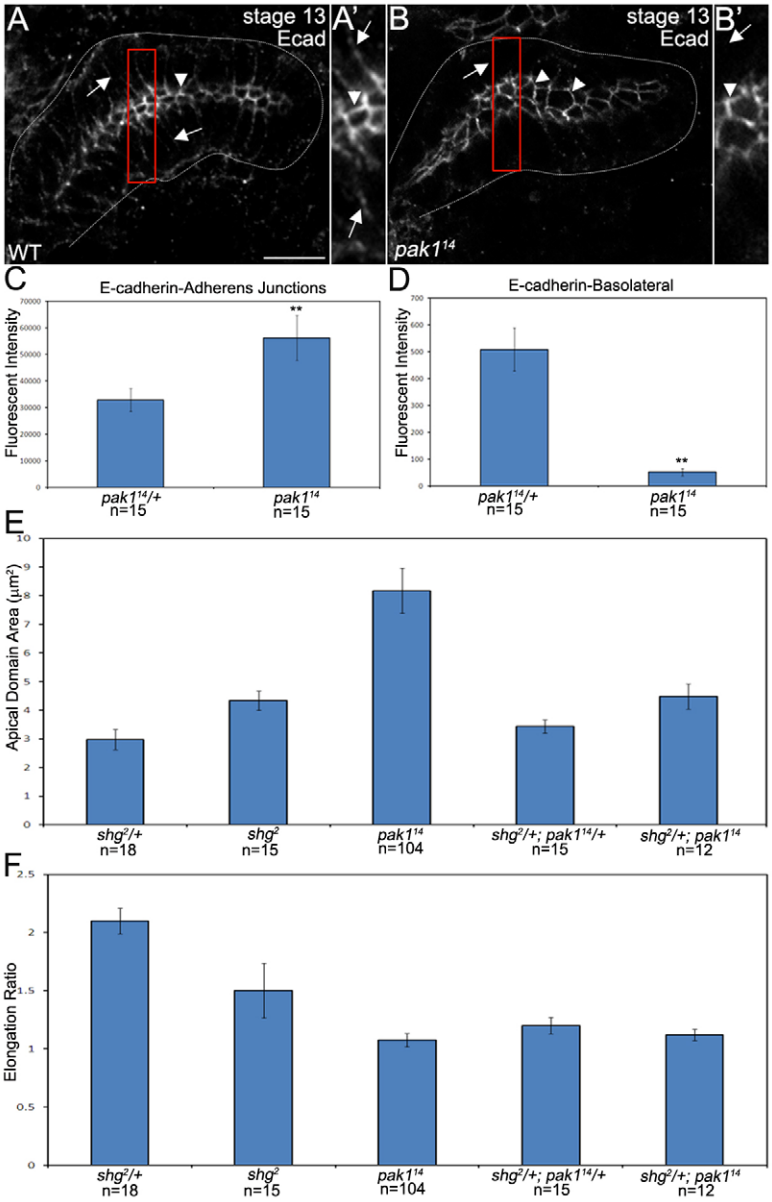

Fig. 2. Pak1 control of apical domain size and elongation is dependent on E-cadherin. (**A-B'**) Embryos stained for E-cadherin (E-cad). Dotted white lines outline the gland. A′ and B′ are enlarged views of regions boxed in A and B, respectively. In *Drosophila* wild-type salivary glands (A,A′), E-cad localizes to the basolateral membrane (arrows) and to adherens junctions (AJs) at the apicolateral membrane (arrowheads). In *Pak1*^{14} mutant glands (B,B′), E-cad was absent from the basolateral membrane (arrows) but still localized to the AJs (arrowheads). (**C**,**D**) Total fluorescence intensity measurements of E-cad at the AJs (C) and at the basolateral membrane (D) in *Pak1*^{14} heterozygous and homozygous embryos. (**E**,**F**) Measurements of apical domain area (E) and elongation ratio (F). *n* represents total number of cells scored per genotype, with three cells measured per gland. Data are mean ± s.d. ***P*<0.0001. Scale bar: 10 μm.

expressing *Rac1*^{DN} (see Fig. S4D in the supplementary material). Measurements of apical domain size and elongation showed that Cdc42 inhibition in the gland resulted in expansion of the apical domain and loss of elongation, similar to that induced by loss of *Pak1* function; however, *Rac1*^{DN} had no effect (see Fig. S4G,H in the supplementary material).

Given the similar gland lumen phenotypes of *Pak1* and *Cdc42* mutant glands, we tested whether Pak1 and Cdc42 could act in a single linear pathway to control lumen size. Inhibition of Cdc42 specifically in glands of *Pak1*^{14} mutant embryos phenocopied inhibition of Cdc42 or loss of *Pak1* alone in terms of gland lumen width, length, apical domain size and elongation (see Fig. S4E-H in the supplementary material), suggesting that Cdc42 and Pak1 act in a single linear pathway. In contrast to Cdc42, expression of *Rac1*^{N17} specifically in *Pak1*^{14} mutant glands decreased lumen length, like inhibition of *Rac1* alone, and widened the lumen, like loss of *Pak1* alone. Thus, simultaneous loss of Rac1 and Pak1 function altered both lumen width and length suggesting that Rac1 and Pak1 act in parallel pathways. Although Cdc42 was shown to affect apical domain size through regulation of the F-actin cytoskeleton in the *Drosophila* notum (Georgiou et al., 2008), F-actin structure in gland cells of *Pak1*^{14} mutant embryos was normal, and embryos mutant for regulators of the actin cytoskeleton, such as WASp, SCAR and Arp2/3 (Arp66B – FlyBase), showed no defects in gland lumen size (data not shown).

Pak1 regulates lumen size and shape through Rab5- and Dynamin-mediated endocytosis

A number of membrane trafficking pathways have been shown to regulate the subcellular localization of E-cad (Delva and Kowalczyk, 2009). For example, E-cad is known to be transported through the recycling endosomes to the plasma membrane in both *Drosophila* and mammalian cells (Desclozeaux et al., 2008; Langevin et al., 2005; Lock and Stow, 2005). In internalized salivary gland cells that are beginning to undergo apical membrane growth and elongation, E-cad localized to the apical membrane and AJs, as well as to discrete puncta at the basolateral membrane with Aval (see Fig. S6A in the supplementary material). Similarly, in

stage 12 wild-type glands when apical domain size was decreasing and elongating, E-cad colocalized with Aval at the AJs, in sub-apical puncta and at the basolateral membrane (see Fig. S6B in the supplementary material). In stage 13 wild-type glands, E-cad continued to localize to puncta at the lateral membrane and at the AJs (see Fig. S6C in the supplementary material). To determine how levels of E-cad at the AJs compared with that at the basolateral membrane, we measured the fluorescence intensity of E-cad at these two locations. Between stages 12 and 13 when the gland turns posteriorly, E-cad levels decreased at the AJs and increased along the basolateral membrane (see Fig. S6D,E in the supplementary material). These data demonstrate that E-cad localization is dynamic during gland turning and suggest that E-cad trafficks through the early endosome during this process.

Since E-cad and Pak1 localized to early endosomes in gland cells (see Figs S5 and S6 in the supplementary material), we tested whether Pak1 could regulate E-cad localization in gland cells through endocytosis. Inhibition of Rab5- or Dynamin-dependent endocytosis, specifically in gland cells, through expression of $Rab5^{S43N}$ (dominant-negative *Rab5*) or shi^{K44A} (dominant-negative *shibire*, the gene encoding Dynamin) resulted in expansion and irregular outpouching of the gland lumen (Fig. 3B,C). Similar lumenal defects were observed in embryos homozygous for a hypomorph allele of *Rab5*, $Rab5^{EY10619}$, and embryos trans-heterozygous for $Pak1^{14}$ and $Rab5^{EY10619}$ (Fig. 3D,F). At the cellular level, apical domains were expanded and not elongated, and E-cad was enhanced at the AJs but reduced or absent at the basolateral membrane of shi^{K44A}- and $Rab5^{S43N}$-expressing gland cells (Fig. 3H,I,M,N; see Fig. S7 in the supplementary material), with the effect of shi^{K44A} being more severe than that of $Rab5^{S43N}$. At the ultrastructural level, the apical surface of shi^{K44A}-expressing gland cells looked identical to that of $Pak1^{14}$ mutant gland cells, in which membrane protrusions into the lumen were absent and instead electron-dense patches at the apical surface membrane were evident (Fig. 1L). To determine to what extent inhibition of endocytosis phenocopied the *Pak1* mutant gland phenotype, we analyzed the effect of reducing *shg* (which encodes E-cad) by half in gland cells expressing shi^{K44A}. Reduction of *shg* levels in glands expressing shi^{K44A} restored the correct apical domain size but had no effect on apical domain elongation (see Fig. S7C,D in the supplementary material). This outcome was identical to the effect of reducing *shg* in $Pak1^{14}$ mutant glands (Fig. 2E,F).

In gland cells of $Pak1^{14}$ homozygous embryos expressing either $Rab5^{S43N}$ ($Pak1^{14}Rab5^{S43N}$) or shi^{K44A} ($Pak1^{14}shi^{K44A}$), specifically in the gland cells, apical domains were expanded and failed to elongate (Fig. 3M,N), and E-cad was absent from the basolateral membrane (data not shown), suggesting that Pak1 acts in a single linear pathway with Rab5 and Dynamin. In contrast to inhibition of Rab5, expression of an activated form of Rab5, $Rab5^{Q88L}$, caused reduction of apical domain size and accumulation of E-cad in sub-apical Aval-positive compartments, compared with wild type (Fig. 3J,M,N; data not shown). Expression of $Rab5^{Q88L}$ in $Pak1^{14}$ mutant gland cells restored apical domain size and elongation, and E-cad localization at the basolateral membrane was similar to that of wild-type gland cells (Fig. 3L,M,N). From these data, we conclude that Pak1 control of Dynamin- and Rab5-dependent endocytosis allows differential localization of E-cad to the AJs and the basolateral membrane, which is important for establishing proper apical domain size and orientation, respectively.

In cultured mammalian cells and in *Drosophila* epithelia, Rab11-dependent recycling of E-cad regulates E-cad localization at the AJs (Delva and Kowalczyk, 2009). To test whether Rab11- or Rab4-dependent recycling could affect E-cad localization at the AJs and/or the basolateral membrane, we analyzed glands expressing dominant-negative *Rab11* ($Rab11^{S25N}$) or dominant-negative *Rab4* ($Rab4^{S22N}$). In contrast to loss of *Pak1* or Shi inhibition, E-cad still localized to the basolateral membrane of gland cells expressing $Rab11^{S25N}$ or $Rab4^{S22N}$ (see Fig. S8B,C in the supplementary material), and in $Rab11^{S25N}$-expressing gland cells we observed an increase in the number of E-cad puncta in the sub-apical region (see Fig. S8C in the supplementary material). Inhibition of either Rab4 or Rab11 doubled apical domain size and only mildly affected apical domain elongation (see Fig. S8D,E in the supplementary material). Thus, in addition to Rab5- and Shi-dependent endocytosis, Rab4- and Rab11-dependent recycling also play a role in determining apical domain size, but do not appear to be required for basolateral localization of E-cad and apical domain elongation.

Pak1 activation promotes E-cadherin endocytosis and formation of multiple lumens

Since our studies of *Pak1* mutant glands indicated a role for Pak1 in E-cad endocytosis, we next tested whether Pak1 activation could enhance E-cad endocytosis. We expressed a dominant active form of Pak1, in which the myristylation sequence of Src1 (Src64B – FlyBase) was fused to the N terminus of Pak1 ($Pak1^{myr}$) (Hing et al., 1999). For gland-specific expression, we used either the second chromosome driver, *fkh*-$GAL4^{II}$, or the third chromosome driver, *fkh*-$GAL4^{III}$, the latter driving higher levels of Pak1 expression compared with the former (see Fig. S9 in the supplementary material). In glands in which $Pak1^{myr}$ was expressed at moderate levels with *fkh*-$GAL4^{II}$, a few intercellular lumens containing the lumen protein Piopio formed at sites of cell-cell contact (Fig. 4B), in contrast to the single continuous lumen of wild-type glands (Fig. 4A). Intercellular lumen formation in $Pak1^{myr}$ glands was preceded by loss of the integrity of the single central lumen. In invaginating control glands, E-cad colocalized with the early endosome markers *Rab5*-GFP (Fig. 4E) and Aval (data not shown) at the apical membrane. In invaginating $Pak1^{myr}$ glands, a single central lumen was no longer apparent; however, strong colocalization of E-cad and *Rab5*-GFP (Fig. 4F), and E-cad and Aval (data not shown) were observed in the disorganized apical domain and in discrete puncta. All apical marker proteins tested, such as Bazooka, Crb and aPKC, and the AJ proteins E-cad and β-catenin, localized to the intracellular vesicles of $Pak1^{myr}$ glands, whereas the basolateral proteins Neurotactin (Nrt) and Discs Large were excluded (data not shown). E-cad was the earliest protein to be internalized in $Pak1^{myr}$-expressing gland cells whereas the localization of Crb remained intact (Fig. 5C). In contrast to the apical membrane, the basolateral membrane did not lose integrity and intracellular vesicles were not observed in the vicinity of the basolateral membrane upon expression of $Pak1^{myr}$ (data not shown).

In glands expressing $Pak1^{myr}$ at high levels with *fkh*-$GAL4^{III}$, formation of multiple lumens was followed by apoptosis and engulfment of gland cells by macrophages (see Fig. S9H,K in the supplementary material). Expression of the baculovirus caspase inhibitor p35 prevented apoptosis of glands induced by $Pak1^{myr}$ (see Fig. S9F,I in the supplementary material). In $Pak1^{myr}p35$ glands, the single continuous lumen became disorganized and was replaced with multiple intercellular lumens in the same temporal manner as glands expressing $Pak1^{myr}$ alone. $Pak1^{myr}$ expression with *fkh*-$GAL4^{III}$ resulted in a more pronounced phenotype, in which the entire gland consisted of multiple intercellular lumens outlined by apical membrane proteins, early endosome marker

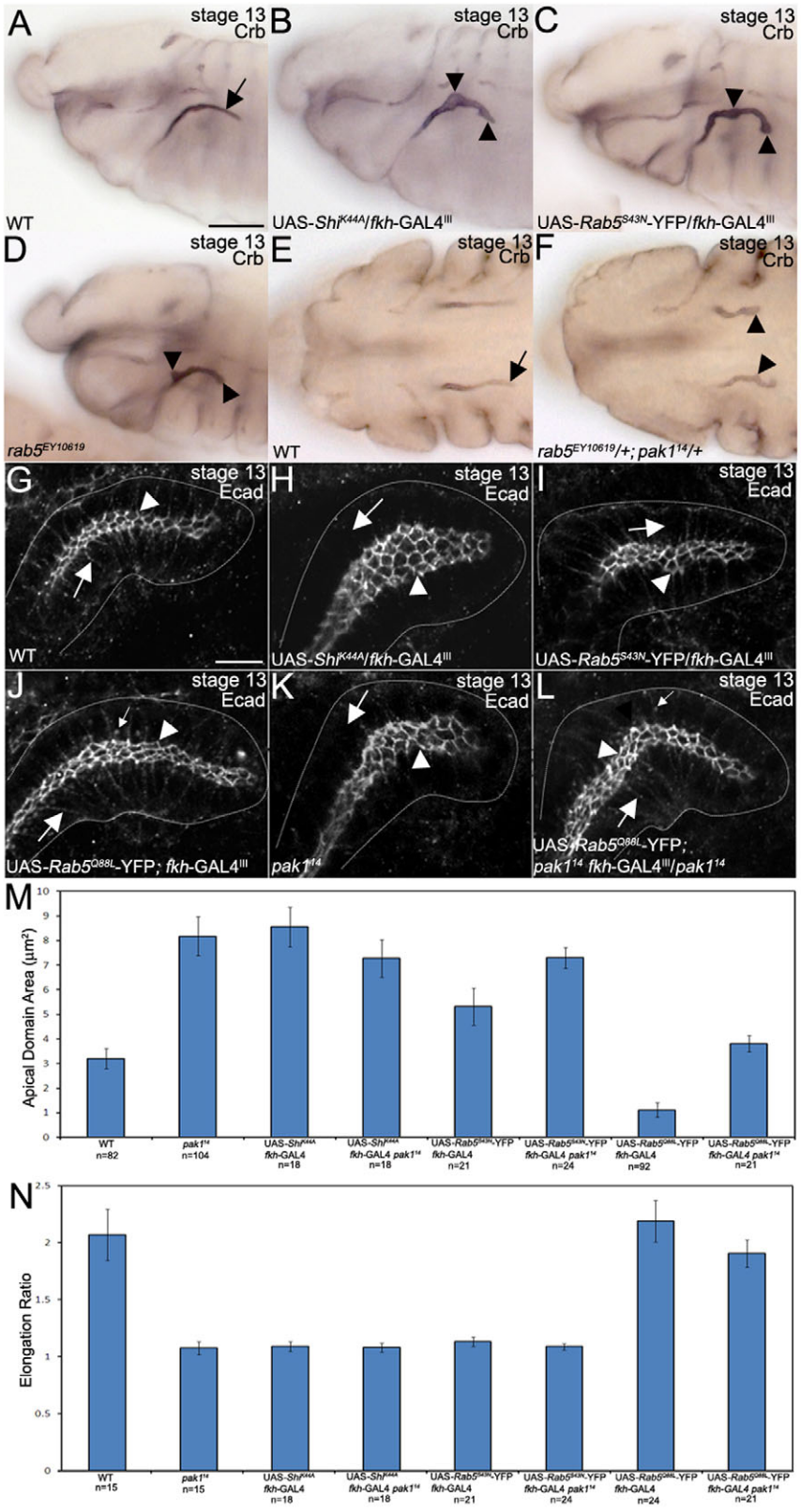

Fig. 3. Endocytosis controls salivary gland lumen size and shape in *Drosophila*.
(**A-L**) Embryos stained for Crb (A-F) and E-cad (G-L). All embryos are lateral views except E and F, which are ventral views. Dotted white lines in G-L outline the gland. Salivary glands of wild-type embryos have lumens of a narrow width (A,E; arrows), whereas those of wild-type embryos expressing *shi*^{K44A} (B) or *Rab5*^{S43N} (C) specifically in the gland with *fkh*-GAL4^{III}, *rab5*^{EY10619} homozygous embryos (D) or *Rab5*^{EY10619};*Pak1*^{14} trans-heterozygous embryos (F) are expanded and irregular in shape (B-D,F; arrowheads). In wild-type glands (G), E-cad localizes to the basolateral membrane (arrow in G) and to the adherens junctions (AJs; arrowhead in G). In glands expressing *shi*^{K44A} (H), E-cad is lost from the basolateral membrane (arrow in H) but is retained at the AJs (arrowhead in H). In glands expressing *Rab5*^{S43N} (I), E-cad at the basolateral membrane is reduced (arrow in I) compared with wild-type glands (arrow in G) but is present at the AJs (arrowhead in I). In glands expressing *Rab5*^{Q88L} (J), E-cad is present at the basolateral membrane (large arrow in J), in the AJs (arrowhead in J) and in enlarged sub-apical puncta (small arrow in J). In *Pak1*^{14} homozygous embryos (K), E-cad is lost from the basolateral membrane (arrow in K) but is present in the AJs (arrowhead in K), whereas in *Pak1*^{14} homozygous embryos expressing *Rab5*^{Q88L} specifically in the gland (L), E-cad is restored along the basolateral membrane (large arrow in L), and in laterally localized puncta (small arrow in L), as well as in the AJs (arrowhead in L).
(**M**,**N**) Measurements of apical domain area (M) and elongation ratio (N). *n* represents the total number of cells scored per genotype, with three cells measured per gland. Data are mean ± s.d. Scale bars: 20 μm in A; 10 μm in G.

proteins and AJ proteins but not basolateral proteins (Fig. 4D and data not shown). We confirmed that the multiple lumens formed by *Pak1*^{myr} were indeed intercellular and not intracellular by TEM, which showed between six and eight cells surrounding a small central lumen in *Pak1*^{myr} *p35*-expressing glands in contrast to wild-type glands, in which the single continuous lumen was surrounded by two rows of cells (Fig. 4G,H). Electron-dense secreted products were found in wild-type and mutant gland lumens demonstrating that loss of normal lumen morphology by *Pak1*^{myr} did not abrogate the gland's secretory function.

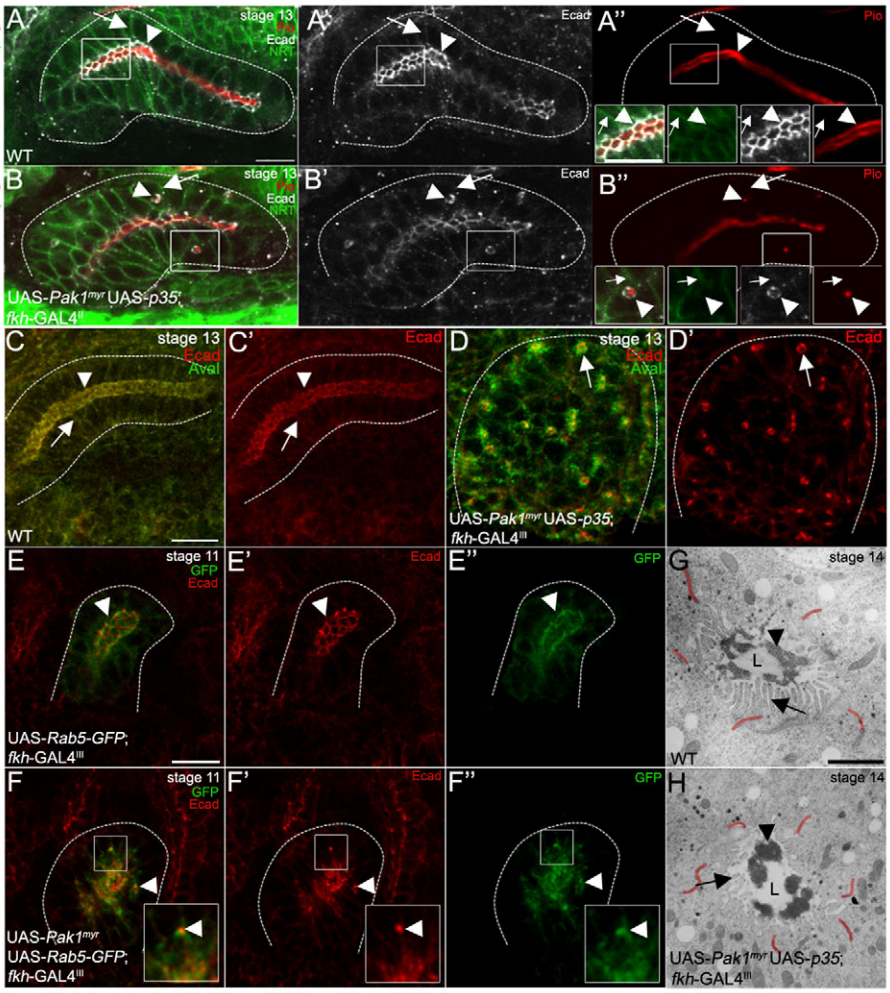

Fig. 4. Pak1 activation causes the formation of multiple intercellular lumens in *Drosophila* salivary glands. (**A-B″**) Triple fluorescence immunostaining of E-cad (white), Neurotactin (Nrt; green) and Pio (red) in salivary glands of stage 13 embryos. For clarity, E-cad staining alone is shown in A′ and B′. Insets in A″ and B″ are magnified views of boxed areas in A and B, respectively. In wild-type embryos (A-A″) salivary glands contain a single continuous lumen filled with Pio whereas E-cad localizes to the apical membrane (arrowheads) and to the basolateral membrane (arrows) labeled with Nrt. In stage 13 embryos expressing *Pak1*^{myr}*p35* specifically in the gland with *fkh*-GAL4^{II} (B-B″), E-cad localized to intercellular lumens (arrowheads) adjacent to the lateral membranes labeled with Nrt (arrows) that contained Pio. (**C-D′**) Double fluorescence immunostaining of E-cad (red) and Avalanche (Aval; green) in salivary glands of stage 13 embryos. For clarity, E-cad staining alone is shown in C′ and D′. In wild-type embryos (C,C′), E-cad colocalizes with Aval at the apical domain (arrowheads) and basolateral membrane (arrows). In stage 13 embryos expressing *Pak1*^{myr}*p35* specifically in the gland with *fkh*-GAL4^{III} (D,D′), E-cad localized to intercellular lumens (arrows) outlined with Aval. (**E-F″**) Double fluorescence immunostaining of E-cad (red) and GFP (green) in salivary glands of stage 11 embryos. For clarity, E-cad staining alone is shown in E′ and F′ and GFP staining alone in E″ and F″. In wild-type embryos expressing wild-type *Rab5*-GFP specifically in the gland (E-E″) E-cad colocalized with *Rab5*-GFP (arrowheads). In *Pak1*^{myr} glands expressing *Rab5*-GFP (F) E-cad colocalized with *Rab5*-GFP in intracellular vesicles (arrowheads). Insets in F-F″ are magnified views of the boxed region in F-F″. Dashed white lines in A-F outline the gland. (**G**,**H**) In stage 14 wild-type embryos (G), microvilli (arrow in G) protrude into the lumen containing electron-dense secretory products (arrowhead in G), whereas *Pak1*^{myr} *p35* glands have fewer and shorter microvilli (arrow in H), although secretory products were found (arrowhead in H). Adherens junctions (AJs) in G and H are marked in red. L, lumen. Scale bars: 10 μm in A,C,E; 5 μm in A″; 1 μm in G.

In *Pak1*^{myr} and control glands, a subpopulation of E-cad colocalized with the late endosome marker, *Rab7*-GFP, in the disorganized apical domain but not in the late endosomes in more basal regions of the cells (see Fig. S10B in the supplementary material). We did not observe colocalization of internalized E-cad with lysosomal protein, *LAMP1* (CG3305 – FlyBase)-GFP (data not shown).

By TEM, we observed membrane-enclosed structures and deep invaginations of the apical membrane in the apical domain of *Pak1*^{myr}*p35* gland cells, in contrast to wild-type cells that had few or none during invagination (see Fig. S11A,B in the supplementary material). Some structures contained cytoplasm enclosed within double membranes, whereas others contained electron-dense materials and vesicles of varying sizes and shapes (see Fig. S11B in the supplementary material). By stage 12, a central lumen was no longer apparent in *Pak1*^{myr}*p35* glands which also lacked membrane protrusions characteristic of those in wild-type glands (see Fig. S11C-E in the supplementary material). Instead, intercellular vesicles surrounded by electron-dense material were apparent in *Pak1*^{myr}*p35* glands (Fig. S11D,E in the supplementary material).

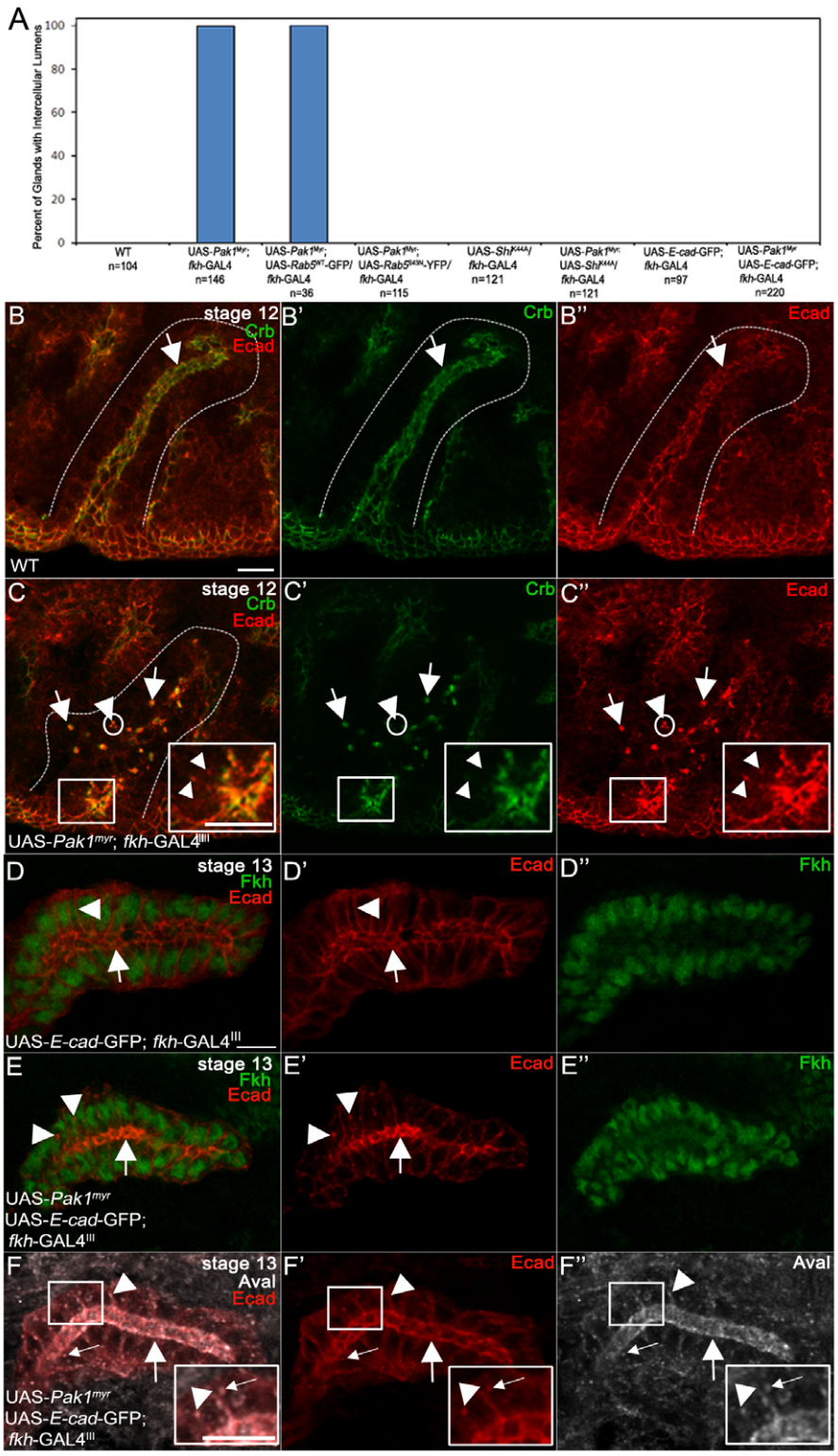

Fig. 5. Multiple lumen formation is dependent on E-cad levels and endocytosis. (**A**) Graph showing percentage of glands with intercellular lumens. *n* represents the total number of glands scored per genotype. (**B-C″**) Double immunostaining for Crb (green) and E-cad (red) in stage 12 *Drosophila* embryos. For clarity, Crb staining alone is shown in B′ and C′ and E-cad staining alone in B″ and C″. In wild-type embryos (B-B″), E-cad and Crb colocalized at the apicolateral membrane (arrows), whereas in embryos expressing $Pak1^{myr}$ specifically in the gland with *fkh*-GAL4^{III} (C-C″), E-cad and Crb colocalized in some intracellular vesicles (arrows) whereas other vesicles contained E-cad but not Crb (arrowheads). Intracellular vesicles containing E-cad (C, red) and not Crb (C, green) are encircled. Insets are enlarged views of the boxed regions in C-C″. (**D-F″**) Double immunostaining for E-cad (red) and either Fkh (D,E; green) or Avalanche (Aval; F; white) in stage 13 embryos. For clarity, E-cad staining alone is shown in D′, E′ and F′; Fkh staining alone in D″ and E″; and Aval staining alone in F″. In embryos expressing wild-type *E-cad*-GFP specifically in the gland with *fkh*-GAL4^{III} (D-D″), E-cad localized to the adherens junctions (AJs; arrows) and the basolateral membrane (arrowheads). In $Pak1^{myr}$ glands expressing wild-type *E-cad*-GFP with *fkh*-GAL4^{III} (E-F″), E-cad localized to the AJs (arrows) and to puncta at the basolateral membrane (arrowheads), and intracellular puncta (small arrows) that co-stained for Aval. Insets are enlarged views of the boxed regions in F-F″. Scale bars: 10 μm in B, D and F.

Pak1 control of lumen size and shape is dependent on E-cad levels and endocytosis

The internalization of apical membrane and AJ proteins into early endosomes in $Pak1^{myr}p35$ glands suggests that endocytosis might play a key role in the formation of intercellular lumens. To test this hypothesis, we inhibited endocytosis by expressing dominant-negative Rab5 ($Rab5^{S43N}$) or dominant-negative Shi (shi^{K44A}) in $Pak1^{myr}$ glands. Expressing $Rab5^{S43N}$ or shi^{K44A} in $Pak1^{myr}$ glands completely inhibited the formation of multiple intercellular lumens, whereas wild-type Rab5 ($Rab5^{WT}$) had no effect (Fig. 5A). By contrast, inhibition of early to late endosome maturation with dominant-negative Rab7 ($Rab7^{T22N}$) or inhibition of early endosome recycling to the plasma membrane with dominant-negative Rab11 ($Rab11^{S25N}$) in $Pak1^{myr}$ glands still resulted in multiple intercellular lumens (data not shown).

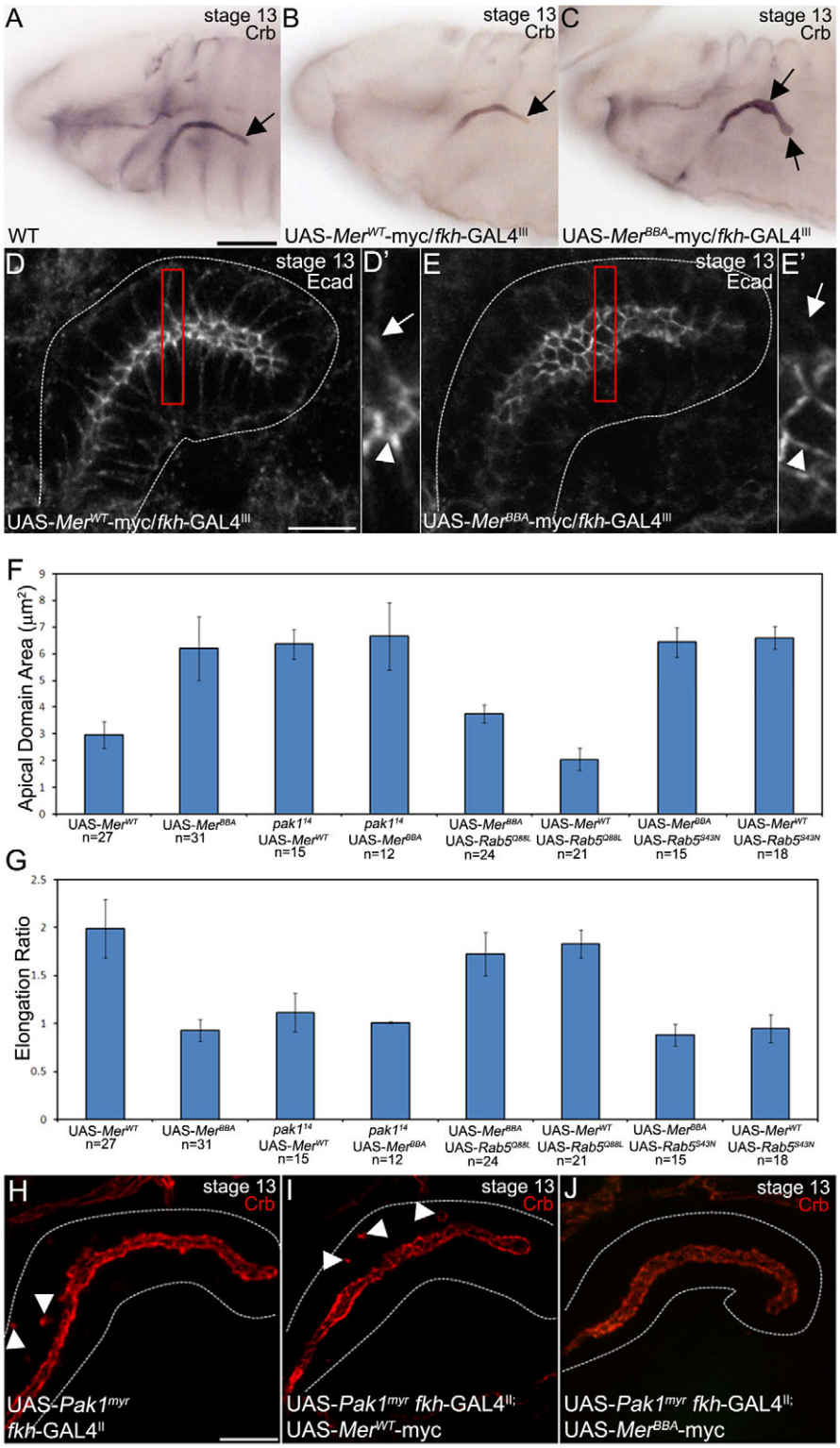

Fig. 6. Merlin regulates salivary gland lumen size downstream of Pak1. (**A-C**) Crb staining in stage 13 *Drosophila* embryos reveals that in wild type (A) the gland lumen (arrows) is similar to that of glands expressing Mer^{WT}-myc specifically in the gland with *fkh*-$GAL4^{III}$ (B), whereas the lumen of glands expressing Mer^{BBA}-myc (C) is expanded and irregular in shape. (**D-E'**) E-cad staining in stage 13 embryos. Red boxes indicate areas enlarged in D′ and E′. In wild-type glands expressing Mer^{WT}-myc (D,D′), E-cad is localized at the adherens junctions (AJs; arrowheads) and the basolateral membrane (arrows), whereas in glands expressing Mer^{BBA}-myc (E,E′), E-cad is localized at the AJs and to a lesser extent at the basolateral membrane. Dotted white lines outline the gland. (**F**,**G**) Measurements of apical domain area (F) and elongation ratio (G). *n* represents total number of cells scored per genotype, with a maximum of three cells measured per gland. Data are mean ± s.d. (**H-J**) Crb staining in stage 13 embryos reveals that glands expressing $Pak1^{myr}$ with *fkh*-$GAL4^{II}$ (H) or co-expressing $Pak1^{myr}$ and Mer^{WT}-myc (I) form intercellular lumens (arrowheads), whereas glands co-expressing $Pak1^{myr}$ and Mer^{BBA}-myc do not (J). Dashed white lines outline the gland. Scale bars: 20 μm in A; 10 μm in D and H.

As E-cad endocytosis in $Pak1^{myr}$glands occurred prior to that of apical membrane proteins, such as Crb (Fig. 5C), we investigated whether expression of wild-type E-cad fused to GFP (*E-cad*-GFP) using a heterologous promoter would be sufficient to prevent multiple lumen formation in $Pak1^{myr}$ glands. Indeed, 100% of $Pak1^{myr}$*E-cad*-GFP glands formed a single central lumen like wild-type glands (Fig. 5A). In the rescued $Pak1^{myr}$*E-cad*-GFP glands, vesicles containing E-cad and Aval but not Crb formed between lateral membranes of neighboring gland cells (Fig. 5E,F); however, such vesicles were not replaced by intercellular lumens (data not shown). Thus, providing excess E-cad in $Pak1^{myr}$ glands was sufficient to prevent activated Pak1 from internalizing AJ and apical membrane proteins and hence prevent multiple lumen formation in the gland. These data indicate that endocytic internalization of E-cad is a key regulatory step in the formation of multiple intercellular lumens.

Merlin is an effector of Pak1 in salivary gland lumen size control

The ERM protein Merlin, also known as Neurofibromatosis 2 (Nf2), is a substrate of Pak1 (Curto and McClatchey, 2008). Merlin localizes to endosomes in cultured Schwann cells (Scoles et al., 2000) and is required for endocytosis of cell surface proteins, including E-cad, in *Drosophila* wing tissue (Maitra et al., 2006). Thus, we tested whether Merlin could be a downstream effector of Pak1 in control of gland lumen size. Gland-specific expression of wild-type Merlin (Mer^{WT}) did not affect gland width; however, expression of dominant-negative Merlin (Mer^{BBA}) (LaJeunesse et al., 1998), expanded the lumen to a degree similar to that observed in *Pak1* and *Rab5* mutant glands (Fig. 6C). Expression of Mer^{BBA} also expanded the apical domain area and reduced the elongation ratio concomitant with loss of E-cad from the basolateral membrane, whereas Mer^{WT} had no effect (Fig. 6D-G). $Pak1^{14}$ mutant glands expressing either Mer^{WT} or Mer^{BBA} still had expanded apical domains that failed to elongate, suggesting that Pak1 and Mer act in a single pathway to regulate apical domain size and shape (Fig. 6F,G). Additionally, co-expression of Mer^{BBA} with $Pak1^{myr}$ prevented the formation of multiple lumens normally observed with $Pak1^{myr}$ alone, whereas co-expression of Mer^{WT} with $Pak1^{myr}$ had no effect (Fig. 6I,J). Thus, normal Merlin activity is required for activated Pak1 to induce E-cad and apical membrane endocytosis and to form intercellular lumens.

To test whether the control of apical domain size by Merlin is dependent on Rab5-mediated endocytosis, we expressed activated *Rab5* ($Rab5^{Q88L}$) or dominant-negative *Rab5* ($Rab5^{S43N}$) simultaneously with Mer^{BBA} specifically in the gland. Co-expression of Mer^{BBA} with $Rab5^{Q88L}$ restored the correct apical domain area and elongation, whereas co-expression of Mer^{BBA} with $Rab5^{S43N}$ had no effect (Fig. 6F,G). Thus, Merlin controls apical domain size and the shape of gland cells in a Rab5-dependent manner.

DISCUSSION

We demonstrate a novel function for *Drosophila* Pak1 in the control of lumen size and shape in the embryonic salivary gland by regulating E-cad localization at the AJs and basolateral membrane through Rab5- and Dynamin-dependent endocytosis. After gland cells have invaginated, they undergo a phase of robust apical membrane growth and apical domain elongation along the Pr-Di

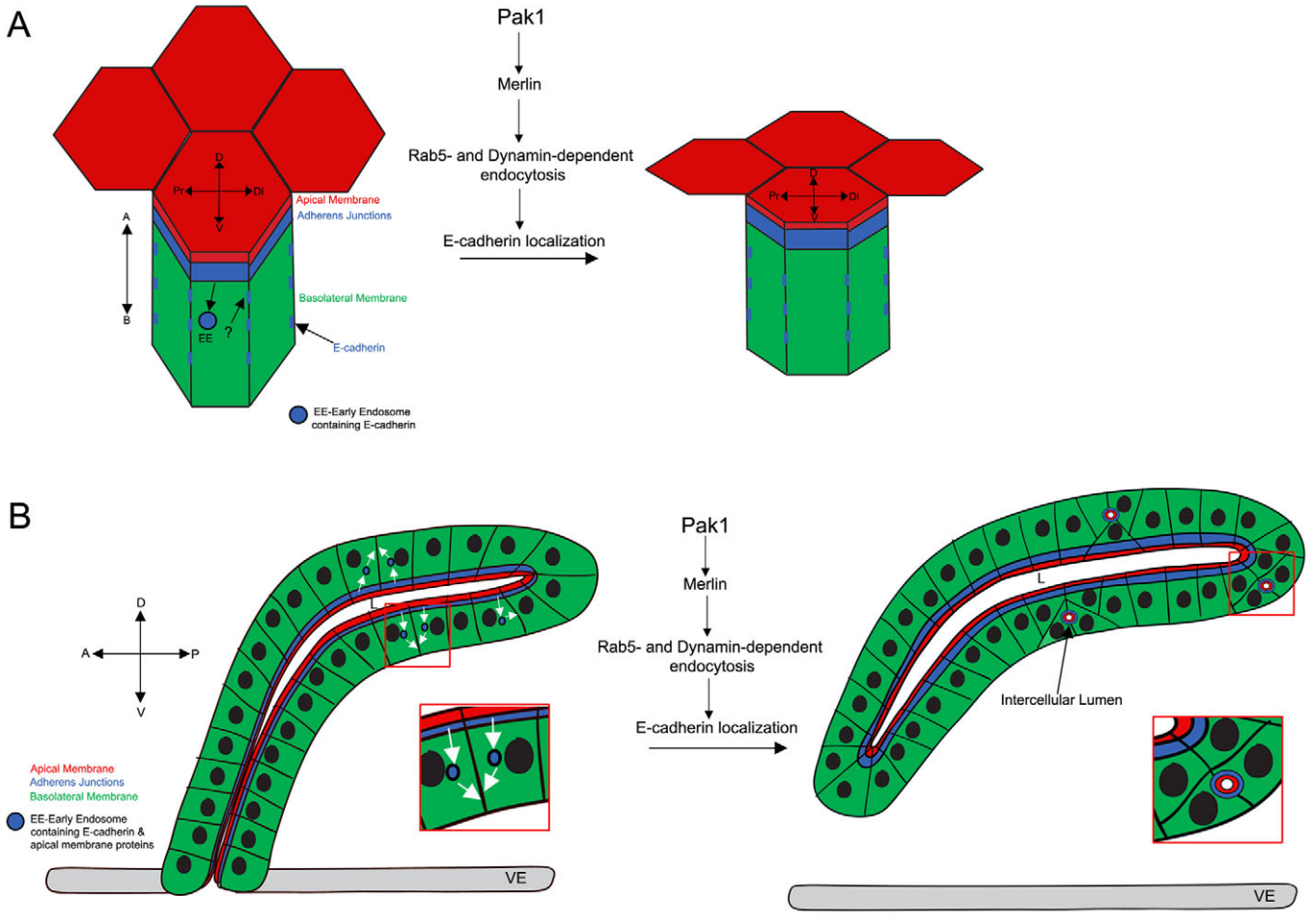

Fig. 7. Model for Pak1 function in salivary gland lumen size control. (**A**) Diagram depicting the lateral view of a gland cell. In wild-type gland cells, Pak1 mediates endocytosis of E-cad from the adherens junctions (AJs) and localization of E-cad to the basolateral membrane, which reduces apical domain size and elongates the apical domain along the Pr-Di axis of the lumen. Pak1 mediates these events through Merlin and Rab5- and Dynamin-dependent endocytosis. A, apical; B, basal; D, dorsal; Di, distal; Pr, proximal; V, ventral. (**B**) Diagram depicting a lateral view of the gland. Constitutively active Pak1 promotes internalization of E-cad and apical membrane proteins into early endosomes, which persist at sites of cell-cell contact and mature into intercellular lumens. This activity of Pak1 is dependent on Merlin, and Rab5- and Dynamin-dependent endocytosis. A, anterior; D, dorsal; P, posterior; L, lumen; V, ventral. Diagrams are not drawn to scale.

axis of the gland. As gland cells turn and migrate, they reduce the size of the apical domain while maintaining its elongated shape. Our studies show that Pak1 regulates apical domain size and elongation during this step through Rab5- and Dynamin-dependent endocytosis of E-cad from the AJs and its subsequent localization at the basolateral membrane (Fig. 7A). A role for Pak1 in the endocytic control of E-cad localization is further supported by our studies with activated Pak1, which demonstrate that Pak1 activation leads to formation of multiple intercellular lumens in addition to, or instead of, a single central lumen (Fig. 7B). Pak1 activation led to Rab5- and Dynamin-mediated endocytosis of E-cad and apical membrane constituents into a single enlarged early endosome located near the cortex of the cell. This cortical early endosome persisted, localized laterally and subsequently expanded to become the new apical domain facing an intercellular lumen between sites of cell-cell contact (Fig. 7B).

Based on our studies, we propose a model for how Pak1 regulation of E-cad controls salivary gland lumen size through modulation of apical domain size and shape. We propose that E-cad destabilization at specific apical interfaces by endocytosis leads to changes in apical tension such that constriction only occurs along the axis of reduced apical tension, i.e. the D-V axis of the apical domains of individual gland cells. This selective constriction of the apical domain then allows the apical domain to elongate and become anisotropic. Pak1 could promote polarized destabilization of E-cad by directly regulating the endocytic machinery or indirectly through the activity of Myosin II and the actomyosin cytoskeleton, which mediates polarized remodeling of E-cad-based cellular junctions during *Drosophila* germband extension (Bertet et al., 2004). Although we did not observe changes in F-actin structure in *Pak1* mutant gland cells and mutations in actin regulators did not perturb gland lumen size, it is still possible that increased localization of E-cad at the AJs in *Pak1* mutant gland cells could lead to an increased apical stiffness, potentially through the association of the AJs with the actin cytoskeleton. Increased apical stiffness could then prevent anisotropic changes of the apical domain. Indeed, previous studies in the *Drosophila* salivary gland have shown that modulation of apical stiffness can result in luminal changes (Cheshire et al., 2008; Kerman et al., 2008).

Recent studies showed a role for the Cdc42-Par-aPKC pathway in E-cad endocytosis from the AJs in *Drosophila* tissues through regulation of the actin cytoskeleton (Georgiou et al., 2008; Leibfried et al., 2008). The E-cad internalization defects reported in these studies differ significantly from data presented here. For example, inhibition of Cdc42 or Dynamin formed disorganized AJs (Georgiou et al., 2008) or large endocytic structures tethered to the AJs (Leibfried et al., 2008), neither of which was observed in Pak1 mutant glands. Moreover, Cdc42 inhibition disrupted F-actin structure (Georgiou et al., 2008), which was also not observed in Pak1 mutant cells. These differences might, in part, be due to tissue-specific requirements for E-cad regulation at different developmental times. In the embryonic neuroectoderm, Cdc42 inhibition leads to loss of apical membrane and AJs proteins, which also contrasts with our findings in *Pak1* mutant glands (Harris and Tepass, 2008). Thus, Pak1 probably controls E-cad endocytosis from the AJs by a mechanism distinct from that of Cdc42 reported in these studies. Based on the studies presented here, we propose that endocytosis in the salivary gland is important for the dynamic localization of E-cad to allow remodeling of the apical domain, which, in turn, is required for achieving proper lumen size and shape.

Our studies provide the first evidence that constitutive activation of Pak1 leads to formation of an epithelial tube with multiple intercellular lumens in a process dependent on endocytosis and E-cad levels. Multiple lumens have been observed during normal organogenesis and in pathological conditions. For example, in the zebrafish intestine, the formation of a tube with a single central lumen is preceded by the formation of multiple intercellular lumens that then coalesce (Bagnat et al., 2007; Horne-Badovinac et al., 2001). In the zebrafish neural tube and *Drosophila* dorsal vessel, Par6γb and Slit regulate single lumen character, respectively (Munson et al., 2008; Santiago-Martinez et al., 2008). Moreover, formation of multiple lumens is a histological feature of breast ductal carcinoma in situ, a pre-invasive form of breast cancer (Debnath and Brugge, 2005). Although a direct role for Pak1-induced endocytosis in these cases of multiple lumen formation has not been demonstrated, it is possible that modulation of cadherin-mediated cell-cell adhesion through membrane transport is a common mechanism by which lumen type and number are determined both in normal developmental processes and in pathological conditions.

Acknowledgements
We thank the many generous members of the fly community, the Bloomington Stock Center and the Developmental Studies Hybridoma Bank for providing fly lines and antisera; D. Andrew, M. Schober and members of the Myat lab for valuable discussions and critical reading of the manuscript; and Lee Cohen-Gould of the Weill Cornell Electron and Confocal Microscopy Facilities and the Rockefeller University Bioimaging Resource Center. This work was supported by NIH grant GM082996 to M.M.M. Deposited in PMC for release after 12 months.

Competing interests statement
The authors declare no competing financial interests.

Supplementary material
Supplementary material for this article is available at
http://dev.biologists.org/lookup/suppl/doi:10.1242/dev.048827/-/DC1

References
Andrew, D., Baig, A., Bhanot, P., Smolik, S. and Henderson, K. (1997). The *Drosophila dCrebA* gene is required for dorsal/ventral patterning of the larval cuticle. *Development* **124**,181-193.
Arias-Romero, L. and Chernoff, J. (2008). A tale of two Paks. *Biol. Cell* **100**, 97-108.
Bagnat, M., Cheung, I., Mostov, K. and Stainier, D. (2007). Genetic control of single lumen formation in the zebrafish gut. *Nat. Cell Biol.* **9**, 954-960.
Bertet, C., Sulak, L. and Lecuit, T. (2004). Myosin-dependent junction remodelling controls planar cell intercalation and axis elongation. *Nature* **429**, 667-671.
Bokoch, G. (2003). Biology of the p21-activated kinases. *Annu. Rev. Biochem.* **72**, 743-781.
Brand, A. H. and Perrimon, N. (1993). Targeted gene expression as a means of altering cell fates and generating dominant phenotypes. *Development* **118**, 401-415.
Buchner, D., Su, F., Yamaoka, J., Kamei, M., Shavit, J., Barthel, L., McGee, B., Amigo, J., Kim, S., Hanosh, A. et al. (2007). Pak2a mutations cause cerebral hemorrhage in *redhead* zebrafish. *Proc. Natl. Acad. Sci. USA* **104**, 13996-14001.
Cheshire, A., Kerman, B., Zipfel, W., Spector, A. and Andrew, D. (2008). Kinetic and mechanical analysis of live tube morphogenesis. *Dev. Dyn.* **237**, 2874-2888.
Colas, J.-F. and Schoenwolf, G. (2001). Towards a cellular and molecular understanding of neurulation. *Dev. Dyn.* **221**, 117-145.
Curto, M. and McClatchey, A. (2008). Nf2/Merlin: a coordinator of receptor signaling and intercellular contact. *Br. J. Cancer* **98**, 256-262.
Damke, H., Baba, T., Warnock, D. and Schmid, S. (1994). Induction of mutant dynamin specifically blocks endocytic coated vesicle formation. *J. Cell Biol.* **127**, 915-934.
Debnath, J. and Brugge, J. (2005). Modelling glandular epithelial cancers in three-dimensional cultures. *Nat. Rev.* **5**, 675-688.
Delva, E. and Kowalczyk, A. (2009). Regulation of cadherin trafficking. *Traffic* **10**, 259-267.
Desclozeaux, M., Venturato, J., Wylie, F., Kay, J., Joseph, S., Le, H. and Stow, J. (2008). Active Rab11 and functional recylcing endosome are required for E-cadherin trafficking and lumen formation during epithelial morphgenesis. *Am. J. Physiol.* **295**, C545-C556.

Georgiou, M., Marinari, E., Burden, J. and Baum, B. (2008). Cdc42, Par6 and aPKC regulate Arp2/3-mediated endocytosis to control local adherens junction stability. *Curr. Biol.* **18**, 1631-1638.
Harris, K. P. and Tepass, U. (2008). Cdc42 and Par proteins stabilize dynamic adherens junctions in the Drosophila neuroectoderm through regulation of apical endocytosis. *J. Cell Biol.* **183**, 1129-1143.
Hing, H., Xiao, J., Harden, N., Lim, L. and Zipursky, S. (1999). Pak functions downstream of Dock to regulate photoreceptor axon guidance in Drosophila. *Cell* **97**, 853-863.
Horne-Badovinac, S., Lin, D., Waldron, S., Schwarz, M., Mbamalu, G., Pawson, T., Jan, Y., Stainier, D. and Abdelilah-Seyfried, S. (2001). Positional cloning of heart and soul reveals multiple roles for PKC lambda in zebrafish organogenesis. *Curr. Biol.* **11**, 1492-1502.
Jaffe, A., Kaji, N., Durgan, J. and Hall, A. (2008). Cdc42 controls spindle orientation to position the apical surface during epithelial morphogenesis. *J. Cell Biol.* **183**, 625-633.
Kamei, M., Saunders, B., Bayless, K., Dye, L., Davis, G. and Weinstein, B. (2006). Endothelial tubes assemble from intracellular vacuoles in vivo. *Nature* **442**, 453-456.
Kerman, B., Cheshire, A., Myat, M. and Andrew, D. (2008). Ribbon modulates apical membrane during tube elongation through Crumbs and Moesin. *Dev. Biol.* **320**, 278-288.
Kiosses, W., Daniels, R., Otey, C., Bokoch, G. and Schwarz, M. (1999). A role for p21-activated kinase in endothelial cell migration. *J. Cell Biol.* **147**, 831-844.
Koh, W., Mahan, R. and Davis, G. (2008). Cdc42- and Rac1-mediated endothelial lumen formation requires Pak2, Pak4 and Par3, and PKC-dependent signaling. *J. Cell Sci.* **121**, 989-1001.
Koh, W., Sachidanandam, K., Stratman, A., Sacharidou, A., Mayo, A., Murphy, E., Cheresh, D. and Davis, G. (2009). Formation of endothelial lumens requires a coordinated PKCepsilon-, Src-, Pak- and Raf-kinase-dependent signaling cascade downstream of Cdc42 activation. *J. Cell Sci.* **122**, 1812-1822.
LaJeunesse, D. R., McCartney, B. M. and Fehon, R. G. (1998). Structural analysis of *Drosophila* Merlin reveals functional domains important for growth control and subcellular localization. *J. Cell Biol.* **141**, 1589-1599.
Langevin, J., Morgan, M., Rosse, C., Racine, V., Sibarita, J.-B., Aresta, S., Murthy, M., Schwarz, T., Camonis, J. and Bellaiche, Y. (2005). Drosophila exocyst components Sec5, Sec6 and Sec15 regulate DE-cadherin trafficking from recycling endosomesto the plasma membrane. *Dev. Cell* **9**, 365-376.
Leibfried, A., Fricke, R., Morgan, M., Bodgan, S. and Bellaiche, Y. (2008). *Drosophila* Cip4 and WASp define a branch of the Cdc42-Par6-aPKC pathway regulating E-cadherin endocytosis. *Curr. Biol.* **18**, 1639-1648.
Liu, J., Fraser, S., Faloon, P., Rollins, E., Vom Berg, J., Starovic-Subota, O., Laliberte, A., Chen, J., Serluca, F. and Childs, S. (2007). A betaPix Pak2a signaling pathway regulates cerebral vascular stability in zebrafish. *Proc. Natl. Acad. Sci. USA* **104**, 13990-13995.
Lock, J. and Stow, J. (2005). Rab11 in recycling endosomes regulates the sorting and basolateral transport of E-cadherin. *Mol. Biol. Cell* **16**, 1744-1755.
Lozano, E., Frasa, M., Smolarczyk, K., Knaus, U. and Braga, V. (2008). PAK is required for the discruption of E-cadherin adhesion by the small GTPase Rac. *J. Cell Sci.* **121**, 933-938.
Lubarsky, B. and Krasnow, M. A. (2003). Tube morphogenesis: making and shaping biological tubes. *Cell* **112**, 19-28.
Mailleux, A., Overholtzer, M. and Brugge, J. (2008). Lumen formation during mammary epithelial morphogenesis: insights from in vitro and in vivo models. *Cell Cycle* **7**, 57-62.
Maitra, S., Kulikauskas, R. M., Gavilan, H. and Fehon, R. G. (2006). The tumor suppressors merlin and expanded function cooperatively to modulate receptor endocytosis and signaling. *Curr. Biol.* **16**, 702-709.
Martin-Belmonte, F. and Mostov, K. (2008). Regulation of cell polarity during epithelial morphogenesis. *Curr. Opin. Cell Biol.* **20**, 227-234.
Martin-Belmonte, F., Gassama, A., Datta, A., Yu, W., Rescher, U., Gerke, V. and Mostov, K. (2007). PTEN-mediated apical segregation of phosphoinositides controls epithelial morphogenesis through Cdc42. *Cell* **128**, 383-397.
Melnick, M. and Jaskoll, T. (2000). Mouse submandibular gland morphogenesis: a paradigm for embryonic signal processing. *Crit. Rev. Oral Biol. Med.* **11**, 199.
Menzel, N., Schneeberger, D. and Raabe, T. (2007). The Drosophila p21 activated kinase Mbt regulates the actin cytoskeleton and adherens junctions to control photoreceptor cell morphogenesis. *Mech. Dev.* **124**, 78-90.
Menzel, N., Melzer, J., Waschke, J., Lenz, C., Wecklein, H., Lochnit, G., Drenckhahn, D. and Raab, T. (2008). The Drosophila p21 activated kinase Mbt modulates DE-cadherin mediated cell adhesion by phosphorylation of Armadillo. *Biochem. J.* **416**, 231-241.
Munson, C., Huisken, J., Bit-Avragim, N., Kuo, T., Dong, P. D., Ober, E. A., Verkade, H., Abdelilah-Seyfried, S. and Stainier, D. (2008). Regulationof neurocoel morphogenesis by Pard6γb. *Dev. Biol.* **324**, 41-54.
Myat, M. M. (2005). Making tubes in the Drosophila embryo. *Dev. Dyn.* **232**, 617-632.
Myat, M. M. and Andrew, D. J. (2002). Epithelial tube morphology is determined by the polarized growth and delivery of apical membrane. *Cell* **111**, 879-891.
Pirraglia, C., Jattani, R. and Myat, M. M. (2006). Rac GTPase in epithelial tube morphogenesis. *Dev. Biol.* **290**, 435-446.
Royal, I., Lamarche-Vane, N., Lamorte, L., Kaibuchi, K. and Park, M. (2000). Activation of cdc42, rac, PAK, and rho-kinase in response to hepatocyte growth factor differentially regulates epithelial cell colony spreading and dissociation. *Mol. Biol. Cell* **11**, 1709-1725.
Santiago-Martinez, E., Soplop, N., Patel, R. and Kramer, S. (2008). Repulsion by Slit and Roundabout prevents Shotgun/E-cadherin-mediated cell adhesion during *Drosophila* heart tube lumen formation. *J. Cell Biol.* **182**, 241-248.
Scoles, D. R., Huynh, D. P., Chen, M. S., Burke, S. P., Gutmann, D. H. and Pulst, S.-M. (2000). The neurofibromatosis 2 tumor suppressor protein interacts with hepatocyte growth factor-regulated tyrosine kinase substrate. *Hum. Mol. Genet.* **9**, 1567-1574.
Strilic, B., Kucera, T., Egliner, J., Hughes, M., McNagny, K., Tsukita, S., Dejana, E., Ferrara, N. and Lammert, E. (2009). The molecular basis of vascular lumen formation in the developing mouse aorta. *Dev. Cell* **17**, 505-515.
Zegers, M., Forget, M., Chernoff, J., Mostov, K., ter Beest, M. and Hansen, S. (2003). Pak1 and PIX regulate contact inhibition during epithelial wound healing. *EMBO J.* **22**, 4155-4165.